Biochimica et Biophysica Acta 1844 (2014) 950–959

Contents lists available at ScienceDirect

Biochimica et Biophysica Acta

journal homepage: www.elsevier.com/locate/bbapap

# Evaluation of reverse phase protein array (RPPA)-based pathway-activation profiling in 84 non-small cell lung cancer (NSCLC) cell lines as platform for cancer proteomics and biomarker discovery ☆

Ramesh Ummanni [a,1,2], Heiko A. Mannsperger [a,2], Johanna Sonntag [a], Marcus Oswald [b,3,4], Ashwini K. Sharma [b,3,4], Rainer König [b,3,4], Ulrike Korf [a,*]

[a] Division of Molecular Genome Analysis, German Cancer Research Center, Im Neuenheimer Feld 580, 69120 Heidelberg, Germany
[b] Integrated Research and Treatment Center, Center for Sepsis Control and Care (CSCC), Jena University Hospital, 07747 Jena, Germany

ARTICLE INFO

*Article history:*
Received 9 April 2013
Received in revised form 4 October 2013
Accepted 13 November 2013
Available online 19 December 2013

*Keywords:*
NSCLC
Cancer genetics
Reverse phase protein arrays
RPPA
Targeted proteomics
Biomarker

ABSTRACT

The reverse phase protein array (RPPA) approach was employed for a quantitative analysis of 71 cancer-relevant proteins and phosphoproteins in 84 non-small cell lung cancer (NSCLC) cell lines and by monitoring the activation state of selected receptor tyrosine kinases, PI3K/AKT and MEK/ERK1/2 signaling, cell cycle control, apoptosis, and DNA damage. Additional information on NSCLC cell lines such as that of transcriptomic data, genomic aberrations, and drug sensitivity was analyzed in the context of proteomic data using supervised and non-supervised approaches for data analysis. First, the unsupervised analysis of proteomic data indicated that proteins clustering closely together reflect well-known signaling modules, e.g. PI3K/AKT- and RAS/RAF/ERK-signaling, cell cycle regulation, and apoptosis. However, mutations of *EGFR*, *ERBB2*, *RAF*, *RAS*, *TP53*, and *PI3K* were found dispersed across different signaling pathway clusters. Merely cell lines with an amplification of EGFR and/or ERBB2 clustered closely together on the proteomic, but not on the transcriptomic level. Secondly, supervised data analysis revealed that sensitivity towards anti-EGFR drugs generally correlated better with high level EGFR phosphorylation than with EGFR abundance itself. High level phosphorylation of RB and high abundance of AURKA were identified as candidates that can potentially predict sensitivity towards the aurora kinase inhibitor VX680. Examples shown demonstrate that the RPPA approach presents a useful platform for targeted proteomics with high potential for biomarker discovery. This article is part of a Special Issue entitled: Biomarkers: A Proteomic Challenge.



## 1. Introduction

Non-small cell lung cancer (NSCLC) presents the most common type of lung cancer, 80–90% of lung cancers are of the NSCLC type while the remaining fraction is small cell lung cancer. The International Agency for Research on Cancer (IARC) reported 1.6 million new NSCLC cases in 2008. Lung cancer still presents a highly fatal cancer with 1.4 million deaths per year [1], and is prevailing as a leading cause of death in economically developed as well as in developing countries. Lung cancer risk factors include smoking and exposure to occupational and environmental carcinogens such as asbestos as well as indoor air pollution from coal-fueled stoves [2,3].

Genetic aberrations such as mutations, gene amplification or deletion of *KRAS*, *EGFR*, *ERBB2*/*HER2*/*neu*, *c-MET*, *LKB1*, *PIK3CA*, *BRAF* and p53 were identified in NSCLC [4,5]. The receptor tyrosine kinase EGFR quickly moved into the focus of drug discovery research and resulted into introducing EGFR targeting drugs such as erlotinib, gefitinib and other compounds into therapeutic regimens. Data on the clinical use of erlotinib and gefitinib demonstrated that both drugs can indeed improve survival [6–8]. Among all reported EGFR mutations especially those of the ATP-binding pocket in the tyrosine kinase domain, initially identified in lung tumors of female patients of East Asian ethnicity without history of tobacco use [9], emerged as a useful predictor of patient response [10–12]. Aiming at the

☆ This article is part of a Special Issue entitled: Biomarkers: A Proteomic Challenge.

* Corresponding author at: Division of Molecular Genome Analysis, B050, German Cancer Research Center (DKFZ), Im Neuenheimer Feld 580, D-69120 Heidelberg, Germany. Tel.: +49 6221 424765; fax: +49 6221 423454.
*E-mail address:* u.korf@dkfz.de (U. Korf).
[1] Permanent address: Center for Chemical Biology, CSIR-Indian Institute of Chemical Technology, Uppal Road, Tarnaka, Hyderabad 500 007, AP, India.
[2] Contributed equally.
[3] Permanent address: Network Modeling, Leibniz Institute for Natural Product Research and Infection Biology, Hans Knöll Institute Jena, 07745 Jena, Germany.
[4] Permanent address: Theoretical Bioinformatics, German Cancer Research Center, INF 580, 69121 Heidelberg, Germany.

http://dx.doi.org/10.1016/j.bbapap.2013.11.017
1570-9639 

identification of genomic markers, a variety of different anti-EGFR compounds has been screened in a large panel of NSCLC cell lines. Vandetanib, lapatinib, the irreversible EGFR inhibitor PD168393, and the src-inhibitor dasatinib revealed similar sensitivity profiles as erlotinib as indicated by a strong correlation with the presence of EGFR mutations in lung cancer cell lines [13,14]. Despite an introduction of highly specific targeted compounds, lung cancer patients are still treated with common cytotoxic drugs and suffer side effects due to nonspecific and unforeseen mechanisms. The identification of reliable biomarker signatures would meaningfully contribute to an improved stratification of lung cancer patients for individualized therapy.

Targeted anti-cancer therapy directly interferes with protein function and for this reason a systematic assessment of protein activation patterns has high potential to result in the identification of new biomarker candidates for further validation. Pathway activation profiling was therefore carried out for >70 cancer-relevant proteins in a panel of 84 NSCLC cell lines to evaluate the potential of reverse phase protein arrays (RPPAs) for cancer biomarker discovery. RPPA is a technically robust experimental platform and produces highly reproducible data guaranteeing comparability between independent printing run and antibody incubations [15,16]. Further properties of RPPA such as high sample capacity, low sample consumption, and high sensitivity qualify this technology for large-scale screening employing clinical specimens as well as cell line panels [17–20]. Technical improvements of the RPPA approach included the introduction of near infrared detection [21] as well as of data analysis tools to yield quantitative information on protein abundance and protein activation [22–24]. However, a successful application of this approach requires access to mono-specific and well-characterized antibodies [25,26].

RPPA-based proteome profiling was centered on detecting the activation state of key signaling players such as of PI3K/AKT/mTOR, RAS/RAF/MEK/ERK, and STAT, as well as additional cancer-relevant pathways such as p53 signaling, apoptosis, and cell cycle control. The NSCLC cell line panel has previously been characterized on the genomic level [27], and genetic aberrations found in this cell line panel have been reported to represent characteristics of primary NSCLC tumors [13]. Transcript profiling was reported not to capture all changes occurring at the cellular level [28] suggesting that a systematic analysis of tumor proteomes can potentially yield valuable insights also for biomarker discovery.

Proteomic data obtained as part of this study were therefore compared with transcriptomic data publicly available for 61 NSCLC cell lines. Besides that, the question whether genetic aberrations directly influence on the regulation of well-known cancer relevant signal transduction circuits was studied in the NSCLC cell line panel. A supervised analysis integrated IC50 data and proteomic data was carried out to yield new insights into drug sensitivity.

## 2. Materials and methods

### 2.1. NSCLC cell lines and protein lysate preparation

Cell lines were obtained from ATCC (American Type Culture Collection), DSMZ (German Collection of Microorganisms and Cell Cultures, Germany), and other cell culture collections as previously described [14]. Information on the cell lines and selected genomic aberrations is provided as part of the Supplementary Table S1. Further information on the assessment of drug sensitivity has previously been described [13]. Cells were regularly tested for mycoplasma contamination using the MycoAlert™ Mycoplasma Detection Kit (Cambrex Bio Science Rockland, Inc., Rockland, ME, USA). Cells were cultivated in RPMI 1640, 10% (v/v) fetal calf serum, 1% (v/v), and Penicillin Streptomycin (100× concentrate) and split twice weekly. For protein lysate preparation, cells were trypsinized, collected and washed two times with PBS. Cell pellets were directly lyzed in MPER buffer (Pierce) with EDTA free complete inhibitors (Roche) and PhosStop (Roche). Lysates were immediately frozen at −80 °C. Further, samples were allowed to thaw on ice and incubated on a rotating shaker at 4 °C for 20 min. To clear protein samples, lysates were centrifuged at maximum speed for 30 min at 4 °C. The protein supernatant was collected and distributed into 3 aliquots for storage at −80 °C until use. Protein concentration was estimated using a micro-BCA method [29].

### 2.2. Targeted proteomics using reverse phase protein array (RPPA)-based profiling

NSCLC cell line samples were printed as four replicate spots per sample using the 2470 Arrayer (Aushon Biosystems, Billerica, U.S.A.) at a total protein concentration pre-adjusted so that 95% of all samples corresponded to a total protein concentration of 2.2 μg/μl, the remaining 5% were at a lower protein concentration. Each array contained in addition serial dilutions of control cell lines serving as quality controls. Slides not used immediately were kept at −20 °C and rehydrated in 0.05% PBS-Tween (w/v) as previously described [21]. Blocking was carried out using Odyssey Blocking buffer (LI-COR, Lincoln, U.S.A.) diluted to 1:1 with 0.05% PBS-Tween (w/v) containing NaF and $NaVO_3$ for 1 h at RT. Next, slides were incubated with pre-validated antibodies (Supplementary Table S2) at 1:300 dilutions in blocking buffer overnight at 4 °C. Antibody validation was carried out by Western blot and only those antibodies giving an explainable band of the expected molecular band were used for RPPA. Control slides were incubated with FAST Green FCF® to determine a spot-specific correction factor [21]. Primary antibody detection was carried out with Alexa 680-labeled secondary antibodies (Molecular Probes, Darmstadt, Germany) diluted 1:8000 and visualized using an Odyssey scanner (LI-COR, Lincoln, USA). Signal intensities were obtained as gpr-files using GenePix Pro 5.0 (Molecular Devices, Ismaning, Germany) [21].

### 2.3. Data analysis

RPPA data analysis was carried out using the software tool RPPanalyzer [23]. Quality criteria were as follows: If serial dilutions of control cell lines did not show a linear correlation between signal intensity and protein concentration, data from the corresponding slide were excluded from further analysis. Antibodies resulting in valid data are listed in Supplementary Table S2. Cut-off for antibody was set to 3-times above blank readings obtained after omitting primary antibodies in the visualization step, readings below this cut-off were considered as equal to 0. In the heatmap (Fig. 1), pairwise Euclidean distances were used together with complete linkage agglomeration to derive a hierarchical clustering of cell lines and proteins of row-normalized data. Correlation coefficients between drug sensitivity and protein expression (Tables 4A/4B) were computed using the Pearson correlation coefficient of the corresponding drug–protein pair yielding values between −1 and +1. We considered a coefficient >0.5 as high correlation, a coefficient between 0.3 and 0.5 as medium and of 0.1–0.3 as a low correlation, correlations were either positive or negative. Protein expression differences between sample groups were calculated using the Wilcoxon rank-sum test and significant differences were calculated at a significance level $\alpha = 0.05$, corrections for multiple testing using the Benjamini–Hochberg algorithm were applied. Overall significance was calculated using the Wilcoxon test and significance was defined as $p < 0.05$.

Gene expression data for 61 NSCLC cell lines was taken from the Cancer Cell Line Encyclopedia (CCLE; http://www.broadinstitute.org/ccle/) [30]. Target proteins used in RPPA were mapped to corresponding genes using BioMart (http://www.ensembl.org/biomart/).

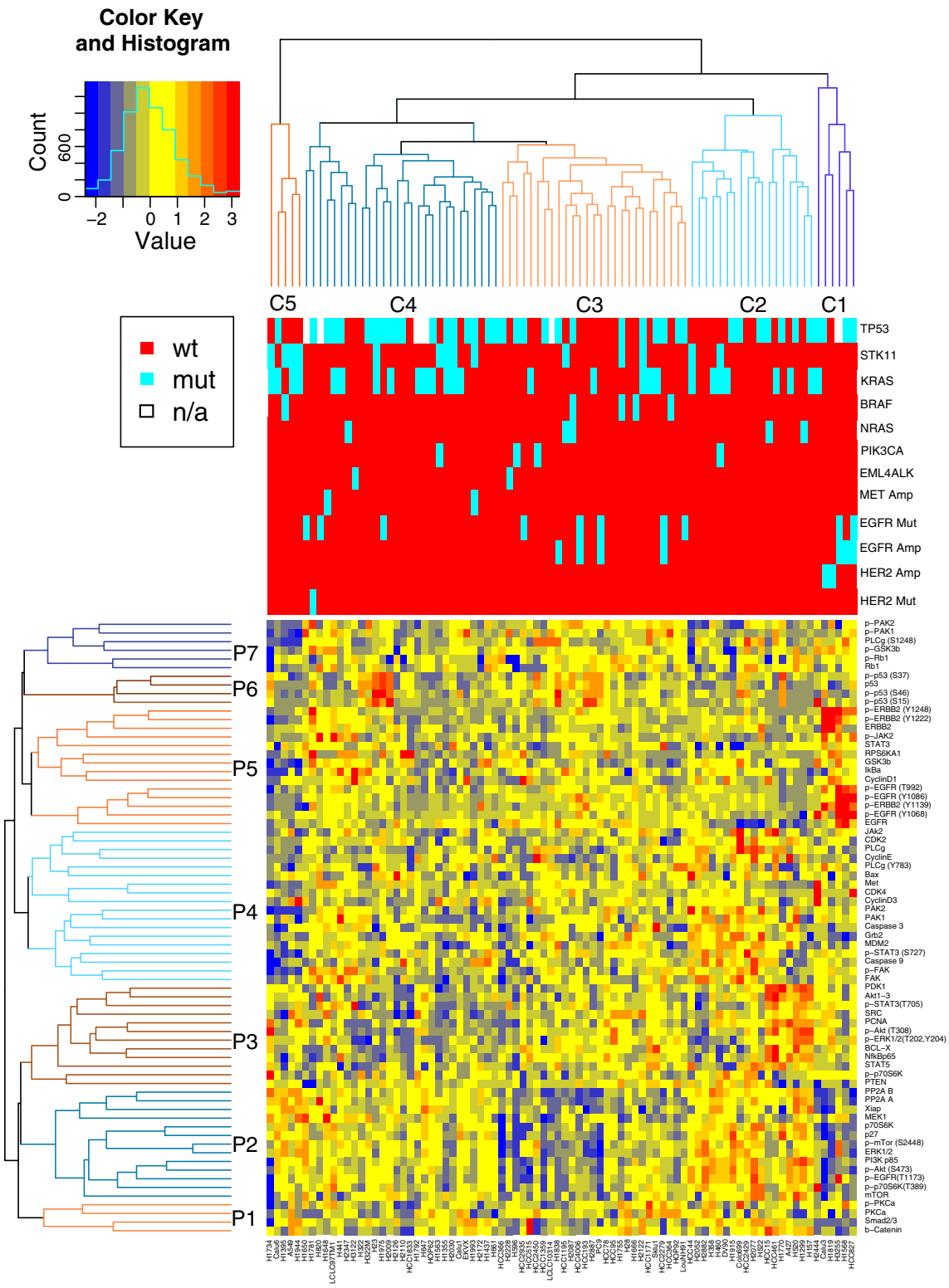


**Fig. 1.** RPPA analysis of 84 non-small cell lung cancer (NSCLC) cell lines. Signal intensities were normalized and log2 converted signals were used for an unsupervised hierarchical cluster analysis. A yellow color indicates that a certain protein matches the medium expression level calculated for a particular target across all cell lines, higher level expression than median is shown as a red color, and a blue color refers to a lower than average abundance (see legend upper left corner). Cell line names and protein names are listed below and on the right-hand side, respectively. Genetic lesions reported for a particular cell line are shown above the heatmap (red indicates *wild type* state of a certain gene, cyan indicates presence of a genomic defect, white indicated that no information was available). Protein clusters (P1 to P7, counted upwards) and cell line clusters (C1 to C5; counted right to left) were visualized as dendrograms. Individual proteins and cell lines of the different clusters are listed in Tables 2A and 2B. All antibodies used for RPPA were validated by Western blot using a subset of randomly chosen cell lines from the NSCLC panel and using established criteria for RPPA. All antibodies are listed in Supplementary Table S2.

The expression data was transformed by dividing the difference from the median values for each gene with its standard deviation. Unsupervised hierarchical clustering using Pearson's correlation and complete linkage method was performed for the cell-lines and the mapped genes. All statistical analyses were done using R (www.r-project.org).

**Table 1**
Genetic aberrations known for the NSCLC panel.

| No. | Name |
|---|---|
| 1 | *EGFR* amplification |
| 2 | *ERBB2* amplification |
| 3 | *MET* amplification |
| 4 | *EGFR* mutation |
| 5 | *ERBB2* mutation |
| 6 | *PI3K* mutation (KD, HD) |
| 7 | *EML4-ALK* fusion |
| 8 | *STK11* mutation |
| 9 | *KRAS* mutation (G12, G13, Q61) |
| 10 | *NRAS* mutation (Q61) |
| 11 | *BRAF* mutation |
| 12 | *TP53* mutation |

**Table 2B**
Heatmap cell line clusters.

| Cluster no. | Cell line |
|---|---|
| C1 | HCC827, H1568, H3255, H1819, Calu3, H2444 |
| C2 | H157,H1299,H520, A427, H1770, HCC461, HCC15, H522, H2077, HCC2429, Colo699, H1915, DV90, H460, H358, H2882, H2052, HCC44 |
| C3 | LouNH91, HOP92, HCC364, HCC2279, Sklu1, HCC171, H2122, H1666, H28, H1755, HCC95, HCC78, PC9, H2887, HCC193, HCC4006, H2087, HCC1195, H1838, LCLC10314, HCC1359, HCC2450, HCC515, HCC2935, H596, H2228, HCC366 |
| C4 | H661, H1437, H2172, H1993, EKVX, Calu1, H2030, H1355, H1563, HOP62, H647, H1792, HCC1833, H2110, H2126, H2009, H1975, H23, H322M, H322, H3122, H2347, H441, LCLC97TM1, H1648, H820, H1781, H1650 |
| C5 | H1944, A549, H1395, Calu6, H1734 |

## 3. Results

### *3.1. Genetic heterogeneity of NSCLC cell lines is reflected in protein composition of cellular proteomes*

Proteomic data were visualized as heatmap after row normalization employing the complete linkage algorithm since this approach agglomerates data as compact clusters that select for a maximal number of common features shared by a large number of cell lines [23]. Signals generated by RPPA are highly reproducible even when slides result from independent print runs and the antibody-based readout was produced on different days (Supplementary Fig. S1). Information on selected genetic lesions reported for the 84 NSCLC cell lines represent both major tumor subtypes of NSCLC, large cell lung cancer and lung adenocarcinoma (Supplementary Table S1). The hierarchy of the NSCLC heatmap obtained this way (Fig. 1) suggested the existence of seven protein clusters (P1 to P7) as well as of five cell line clusters (C1–C5). First of all, proteome clusters contained mostly proteins known as functionally related representing different members of a certain signaling pathway (Table 2A) such as proteins of the PI3K/AKT/mTOR signaling module (P2), proteins involved in the regulation of cell cycle and apoptosis (P4), receptor tyrosine kinases (P5), p53 signaling (P6), and GSK3 signaling (P7). Proteome cluster P3 included a more heterogeneous set of target proteins and contained proteins typically associated with the initial steps of the PI3K/AKT signaling pathway such as PDK1, PTEN, and pAKT (T308) as well as proteins of the MEK/ERK pathway and of the NFκB/STAT signaling circuit. Cluster P1 contained β-Catenin and Smad2/3 as well as PKCα and phosphorylated PKCα. The Pearson correlation coefficient between single proteomic clusters was generally <0.3 indicating an independent regulation of pathway-specific clusters.

We next assessed proteomic data with respect to the question, how individual genetic lesions (Table 1) e.g. mutated *KRAS* and *TP53* and mutations or amplifications of *ERBB2* or *EGFR* influence the activation state of downstream signaling pathways. Three of seven *EGFR* amplified cell lines (H3255, H1568, HCC827) as well as both ERBB2 amplified NSCLC cell lines, Calu3 and H1819, formed a single cell cluster along with H2444 cells that did not carry an amplification of EGFR or ERBB2 (C1). Five C1 cell lines were characterized by either high levels of ERBB2 and/or EGFR and by high level phosphorylation of ERBB2 (Y1222, Y1248) and/or of EGFR (Y992, Y1068, Y1086, and Y1139). Moreover, all six C1 cell lines expressed low levels of β-Catenin and SMAD2/3 (P1) and showed also low level activity of the PI3K/AKT/mTOR signaling axis (P2). Co-occurrence of β-Catenin and SMAD2/3 was highly correlated in the NSCLC cell line panel according to a Pearson correlation factor of 0.721 ($p < 0.0001$). Four further NSCLC cell lines with amplified *EGFR* (H1838, HCC2279, HCC4006, PC9) were part of cell line cluster C3 that, contrasting cluster C1, did not display high level phosphorylation of EGFR or ERBB2. Other features of C1, such as low level activity of the AKT signaling module and low level expression of β-Catenin/SMAD2/3 were also seen in C3. Cell line cluster C2 reflected high level activation of PI3K/mTOR signaling (P2), low level abundance of EGFR and ERBB2 (P5) and a heterogeneous activation pattern for other signaling proteins. Interestingly, cell lines assigned to the squamous cell carcinoma subtype or to mesothelioma were found in C2 and C3 but in none of the other cell line cluster. Cell lines with low level activation of AKT/ERK signaling (P3) and divergent abundance for proteins of the p53 cluster (P2) were assigned to cluster C4 which includes also both MET amplified cell lines of the NSCLC panel, H1648 and H1993. Cluster C5 comprised only few cell lines characterized by low level abundance of proteins representing the apoptosis/cell cycle control cluster (P4) and the pGSK3β/pRB cluster (P7) along with high level activation of AKT pathway proteins. Next, proteomic clusters were compared with results obtained from an unsupervised analysis of expression profiling data of 62 NSCLC cell lines that were available from the Cancer Cell Line Encyclopedia (CCLE) [30] using row normalization and complete linkage. Comparable to the proteomic heatmap, many proteins of known and well-described signaling pathways clustered together as, for example, transcripts coding for proteins involved in mediating inflammatory response such as members of NFκB/STAT signaling (Supplementary Fig. S2). However, unlike the very homogenous pathway activation cluster found for cell lines with an amplification of the *EGFR* or *HER2* gene (HCC827, H2444, Calu3, H3255, H1568) no tight

**Table 2A**
Heatmap protein clusters.

| Cluster no. | Target proteins |
|---|---|
| P1 | Smad2/3, β-Catenin, PKCα, pPKCα |
| P2 | mTOR, pmTOR (S2448), p70S6K, pp70S6K(T389), pAKT(S473), PI3Kp85, p27, MEK, PP2A, PP2B, PTEN |
| P3 | STAT5, pSTAT3 (T705), NFκB, BCL-X, pERK1/2(T202/Y204), AKT, pAKT(T308), PDK1, PCNA, SRC, pFAK |
| P4 | FAK, Caspase9, Caspase 3, pSTAT(S727), MDM2, GRB2, PAK1, PAK2, cyclin D, cyclin E, CDK2, CDK4, JAK2, MET, BAX |
| P5 | EGFR, pEGFR (Y 992, 1068, 1086, 1139), cyclinD1, IKBα, GSK3β, STAT3, pJAK2, ERBB2, pERBB2 (Y1222, Y1248) |
| P6 | p53, p53(S15), p53(S48), p53 (S37) |
| P7 | RB1, pRB1, pGSK3β, PLCγ(S1248), pPAK1, pPAK2 |

**Table 3**
Targeted drugs tested in the NSCLC panel.

| No | Name | PubChem no. |
|---|---|---|
| 1 | Erlotinib | 176870 |
| 2 | Vandetanib | 3081361 |
| 3 | Dasatinib | 3062316 |
| 4 | PD168393 | 26759325 |
| 5 | Lapatinib | 208908 |
| 6 | VX680 | 5494449 |

**Table 4A**
Correlation between drug sensitivity and EGFR/ERBB2 activation state (p-value (top), correlation value in *italics* (below)).

| | | ERBB2 | pERBB2 Y1222 | pERBB2 Y1139 | pERBB2 Y1248 | EGFR | pEGFR Y1086 | pEGFR Y1068 |
|---|---|---|---|---|---|---|---|---|
| 1 | Erlotinib | ns | 0.012<br>*−0.35* | 0.015<br>*−0.31* | 0.009<br>*−0.38* | 0.023<br>*−0.29* | 0.013<br>*−0.32* | 0.009<br>*−0.32* |
| 2 | Vandetanib | ns | ns | ns | ns | 0.038<br>*−0.26* | 0.016<br>*−0.30* | 0.012<br>*−0.33* |
| 3 | Dasatinib | ns | ns | ns | ns | ns | ns | ns |
| 4 | PD168393 | ns | 0.017<br>*−0.30* | 0.014<br>*−0.32* | 0.013<br>*−0.32* | ns | 0.023<br>*−0.28* | 0.013<br>*−0.32* |
| 5 | lapatinib | 0.027<br>*−0.27* | 0.004<br>*−0.42* | 0.009<br>*−0.36* | 0.004<br>*−0.42* | ns | 0.014<br>*−0.32* | 0.033<br>*−0.26* |
| 6 | VX680 | 0.009<br>0.37 | ns | ns | ns | ns | ns | ns |

ns = no significant p-value, in this case correlation factor not listed. Correlation (Pearson) <0.3 indicates low level correlation, above 0.5 a high correlation and 0.3–0.5 average correlation. p-values were Benjamini–Hochberg-corrected, data for GSK3b and CyclinD1 were omitted since no significant correlation with drug resistance was observed.

clustering was observed on the transcript level for this particular set of cell lines (Supplementary Fig. S2).

### 3.2. Pathway activation clusters do not reflect TP53 mutations

Mutations of *TP53* were present in 43 NSCLC cell lines (Supplementary Table S1). Two hot spots of high level p53 phosphorylation were noted (cluster P6, Fig. 1) that apparently correlated with a low level phosphorylation of AKT on S473. The first hot spot contained five cluster C4 cell lines that showed only a weak negative correlation with AKT signaling whereas the second hotspot, located within the C3 cluster, revealed a weak negative correlation of −0,206 after omitting p70S6K data since this protein positively correlated with p53 abundance. To evaluate observations made by RPPA, selected cell lines were analyzed by Western blot. Cell lines were chosen from both clusters with high level p53 phosphorylation (H23, H2887, PC9), H157 cells representing low level p53 expression were included as negative control. High level expression of p53 and high level phosphorylation of p53 were confirmed by Western blot for the *wt TP53* cell lines PC9 and H2887 of cluster C3 as well as in the *wt TP53* cell line of cluster C4 (H23) whereas the control cell line H157 cells showed low levels of p53 as well as low level p53 phosphorylation (Fig. 2). The AKT activation state was apparently lower in cell lines selected from p53 hot spot clusters compared to H157 cells that showed also higher levels of total AKT. Besides that, PTEN expression was higher in the three p53 hot spot cell lines when analyzed by Western blot. Findings made with respect to the PTEN expression are not fully in accordance with RPPA data. Reasons for this incoherent PTEN determination might be due to the fact that dynamic range and signal normalization of RPPA and Western blot are very different which affects small differences more strongly than large differences.

**Table 4B**
Correlation between drug sensitivity and activation state of different signaling modules (p-value (top), correlation value in *italics* (below).

| | | PP2A/ A | PP2A/ B | p70S6K | PI3K/ p85 | p27 | Smad 2/3 | pAkt* | pEGFR Y992 |
|---|---|---|---|---|---|---|---|---|---|
| 1 | Erlotinib | ns | ns | 0.003<br>*0.46* | 0.03<br>*0.38* | 0.005<br>*0.42* | ns | ns | 0.015<br>*−0.31* |
| 2 | Vandetanib | ns | ns | 0.005<br>*0.39* | 0.04<br>*0.36* | 0.03<br>*0.34* | ns | ns | 0.03<br>*−0.26* |
| 3 | Dasatinib | 0.029<br>*0.26* | 0.005<br>*0.36* | 0.01<br>*0.30* | 0.03<br>*0.33* | 0.009<br>*0.30* | 0.03<br>*0.25* | ns | ns |
| 4 | PD168393 | 0.029<br>*0.28* | 0.012<br>*0.33* | 0.03<br>*0.30* | *ns* | 0.03<br>*0.33* | ns | ns | 0.015<br>*−0.31* |
| 5 | Lapatinib | ns | ns | ns | ns | ns | ns | *ns* | 0.02<br>*−0.31* |
| 6 | VX.680 | ns | ns | ns | *ns* | *ns* | ns | ns | ns |

ns = no significant p-value, in this case correlation factor not listed; * pAKT (S473). Correlation (Pearson) <0.3 indicates low level correlation, above 0.5 a high correlation and 0.3–0.5 average correlation, p-values were Benjamini–Hochberg-corrected.

### 3.3. Impact of KRAS mutations on NSCLC signaling networks

The NSCLC cell line panel included 26 *KRAS*-mutated NSCLC cell lines and five cell lines with mutated *NRAS or BRAF*. Of the 26 *KRAS*-mutations, 18 affected codon G12, six mutations were identified in codon G13, and only two in codon Q61. Mutations of *KRAS*, NRAS, and *BRAF* revealed little impact on the protein heatmap hierarchy (Fig. 1). This suggests that mutations of *KRAS*, *NRAS*, and *BRAF* either affect downstream signaling circuits in either a rather subtle way or differ in their outcome. Protein activation states were therefore analyzed by supervised learning and limited to the analysis of *KRAS* mutations on signaling. The resulting data revealed that cell lines with mutated *KRAS* expressed significantly elevated levels of certain proteins, such as PP2A, and contained also higher levels of pAKT (S473) and pp70S6K but lower levels of pPLCγ (S1248) when compared to *wt KRAS* cell lines (Fig. 3). Phosphorylation of p53 was also lower in KRAS mutated cell lines but not quite meeting our significance criteria ($p = 0.053$).

### 3.4. Protein profiling data identify drug resistance mechanisms

Proteomic profiles obtained for the NSCLC cell line panel were analyzed and visualized in two different ways employing IC50 values available for drugs targeting cancer-relevant kinases, e.g. EGFR, ERBB2 and aurora kinase A (Table 3, Supplementary Table S3) [13,14]. Firstly, the Pearson correlation coefficient was computed for all possible drug–protein pairs to identify potential correlations between drug sensitivity and protein abundance. Expression levels of proteins correlating significantly with drug response (Tables 4A and 4B) and IC50 values of selected drugs were visualized as scatter plots (Supplementary Fig. S3). For all EGFR inhibitors, receptor phosphorylation was a better indicator of drug sensitivity than the expression level of the receptor itself (Table 4A). Sensitivity towards lapatinib correlated best with high level ERBB2 (Y1248) phosphorylation ($p = 0.004$) and, as seen before for EGFR inhibition, receptor phosphorylation was superior as readout when compared to the ERBB2 total protein level ($p = 0.027$). According to our data, sensitivity towards the BCR-ABL and SRC inhibitor dasatinib showed specificity towards expression of proteins downstream of EGFR/ERBB2 (Table 4B) but not so towards expression level or activation of EGFR or ERBB2 (Table 4B). Sensitivity towards dasatinib seemed to be higher in cell lines with low level expression of SMAD2/3. Cell lines sensitive towards the EGFR-targeting drug erlotinib were characterized by a significantly higher phosphorylation of EGFR on Y1086 ($p = 0.013$), Y1068 ($p = 0.009$), and pERBB2 (Y1248) ($p = 0.015$) (Fig. 4). In addition, erlotinib-sensitive cells showed reduced expression of proteins involved in PI3K/AKT/p70S6K signaling (Table 4B), a feature noticed also for vandetanib, dasatinib, and PD168393 but not so for lapatinib. Sensitivity towards targeted EGFR inhibitors correlated with low abundance of PP2A subunits. Low level expression of PP2A was noticed for cells responding to PD168393, an irreversible inhibitor of EGFR and ERBB2.

Few NSCLC cell lines, e.g. H157, HCC2429, and A427 revealed high sensitivity towards the aurora kinase inhibitor VX680 which abrogates aurora kinase function and disturbs the segregation of chromosomes during mitosis [31]. However, high level AKT signaling was a characteristic for VX680 responsive cells. Expression levels of other cell cycle proteins not probed by RPPA were re-assessed by Western blot in a VX680-sensitive cell line, in a VX680-resistant cell line and in two cell lines of intermediate sensitivity towards VX680. Western blot data indicated that VX680-sensitive cells indeed express aurora kinase A (AURKA) at a high level, an M-phase associated protein, and showed a strong

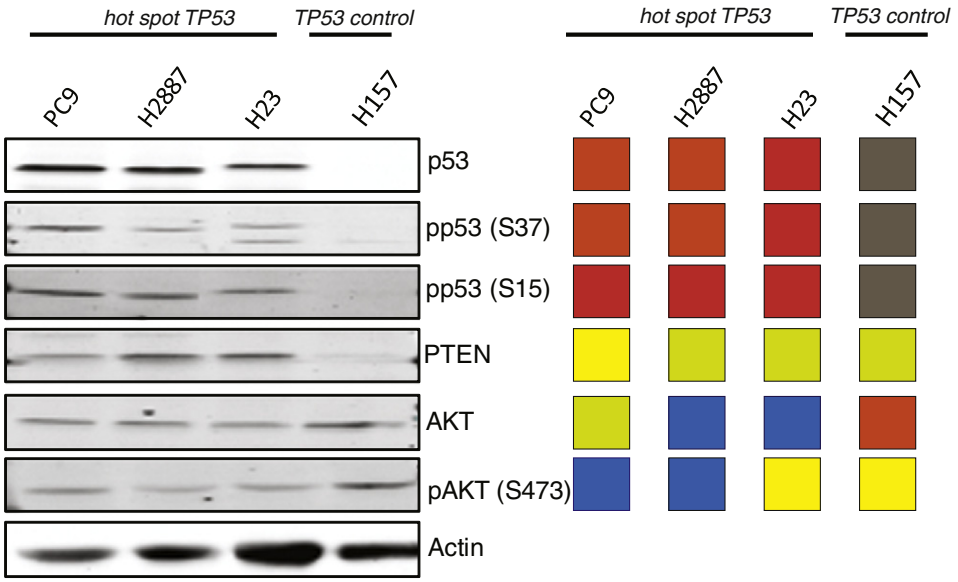


**Fig. 2.** Evaluation of p53 hot spots by Western blot. Cell lines were chosen from the two hot spots of Fig. 1 showing high level p53 activation (PC9, H2887, H23) and H157 as control since it shows low level p53 phosphorylation. Cell lines express *wt TP53* (PC9, H2887) or mutated *TP53* (H157, H23). RPPA data were normalized based on total protein content and signals were row-normalized and colors taken from Fig. 1. For Western blots equal amounts of cell lysates (20 μg total protein) were loaded per lane. p53 expression was detectable in all hot spot cell lines as well as phosphorylation of p53, AKT expression was higher in H157 cells.

phosphorylation of RB indicative of a transitional cell cycle state. Typical G1-phase proteins such as CDK4 and cyclin D and the G2/M-phase protein cdc2 (CDK1) were lowly expressed in VX680 sensitive cells, cyclin B expression was comparable to other cell lines (Fig. 5). VX680 resistant cells expressed low levels of aurora kinase and showed low level RB phosphorylation.

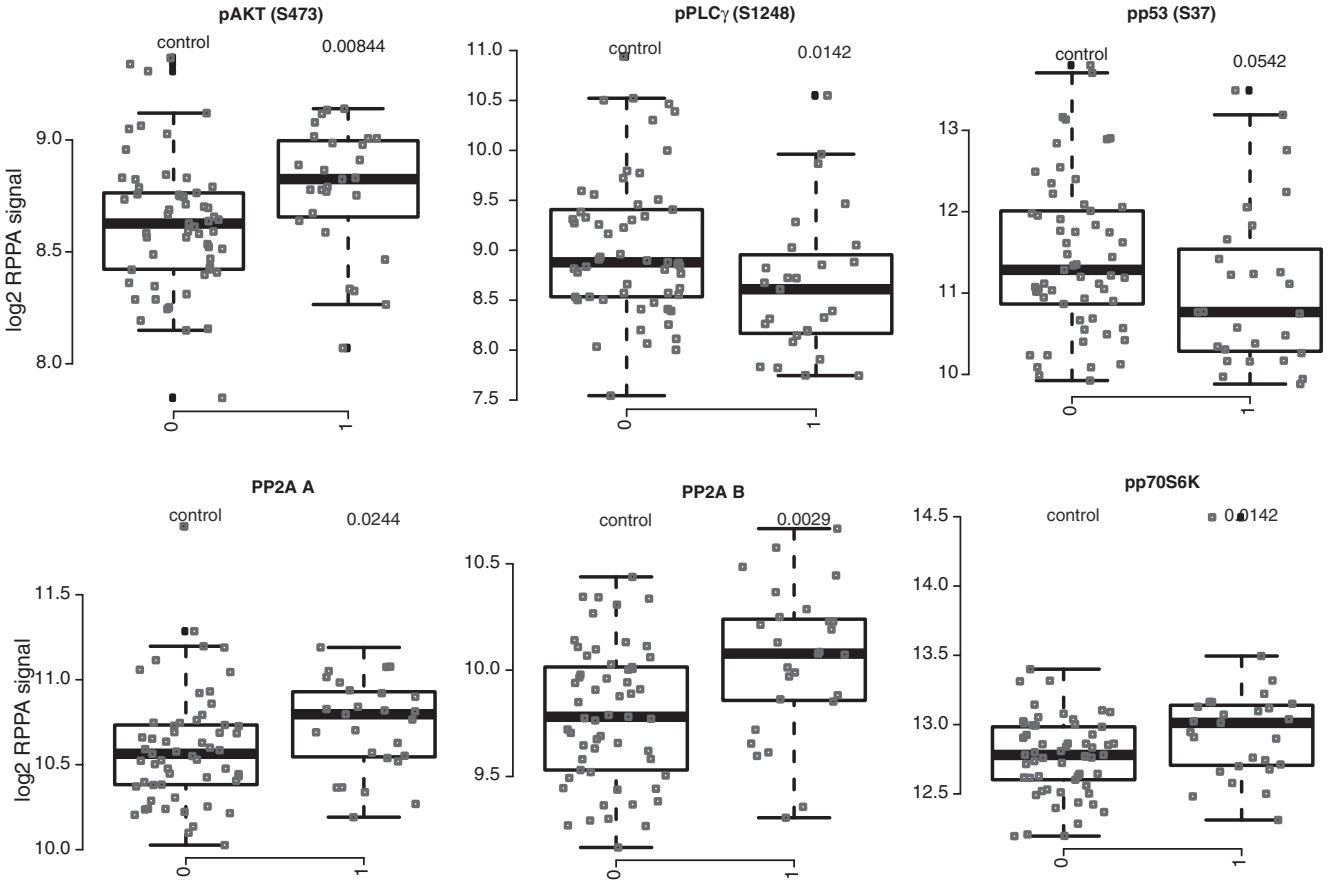


**Fig. 3.** Impact of *KRAS* lesions on signaling. AKT (S473) phosphorylation, PP2A subunits A and B, and pp70S6K (T389) are upregulated whereas ppPLCγ (S1248) and pp53 (S37) were downregulated in *KRAS*-mutated NSCLC cell lines. Proteomic data obtained for cell lines listed in Supplementary Table S1 as *KRAS* (G12, G13, Q61) were compared with those of *wt KRAS* cell lines using supervised clustering. Proteins corresponding to highly differential expression are represented as box-plot diagrams after log2 transformation of normalized RPPA signals, p-values (Wilcoxon) are shown above box-plots.

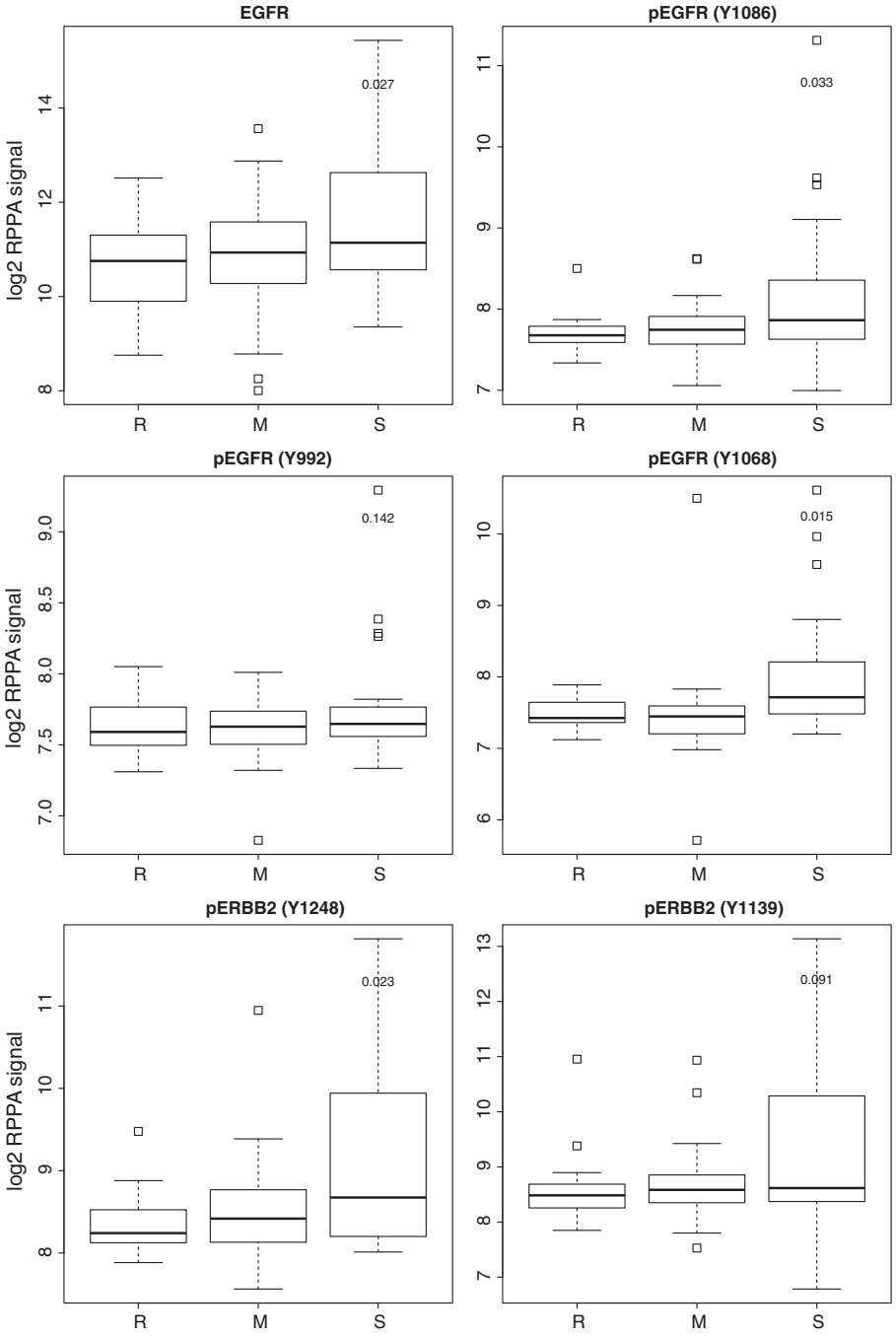


**Fig. 4.** Correlation between erlotinib sensitivity and protein expression. Erlotinib-sensitive cell lines are indicated as (S) and represent the lower quartile of IC50-values. RPPA signals were log2 transformed, p-values (Wilcoxon) are shown above box-plots for the comparison between resistant cells and sensitive cells. Erlotinib-resistant cell lines (R) represent the highest quartile of IC50-values, the two quartiles representing cell lines with an intermediate sensitivity are shown as (M). Sensitivity towards erlotinib correlates best with high level EGFR or ERBB2 receptor phosphorylation, e.g. with an increased phosphorylation of EGFR on Y1068 ($p = 0.015$) and on Y1086 ($p = 0.033$), of ERBB2 on Y1248 ($p = 0.023$) and with total EGFR levels ($p = 0.027$). Other EGFR phosphorylation sites (Y992 and Y1191) did not show a significant correlation with sensitivity. No significant correlation with respect to receptor phosphorylation was observed for the comparison between the groups (R) and (M).

Integration of proteomic data and IC50 data suggests that RPPA-based pathway activation profiling presents a useful platform to identify new biomarker candidates. For example, the EGFR phosphorylation on Y1068 presents a useful indicator of sensitivity towards EGFR-targeting drugs. Dasatinib seems to be more specific to inhibit EGFR than erlotinib, vandetanib and PD168393 since no significant correlation with ERBB2 phosphorylation was seen. A prominent indicator of sensitivity towards EGFR-targeting drug PD168393 is apparently the expression of the protein phosphatase PP2A. In turn, promising candidates of sensitivity towards VX680 are aurora kinase expression in conjunction with assessing the RB phosphorylation state. To sum up, diverse patterns of cellular regulation observed in the NSCLC cell line panel illustrate its molecular heterogeneity and the need for patient-tailored therapies.

## 4. Discussion

Multiple signaling pathways are known to be involved in the initiation and progression of lung cancer [32–34]. In the clinics, treatment of NSCLC patients with targeted drugs aiming at the inhibition of EGFR

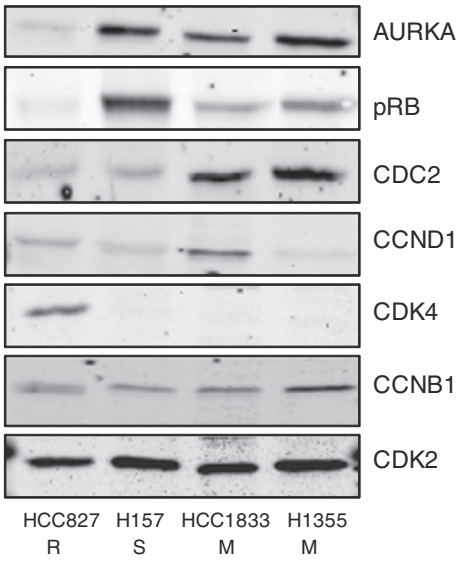


**Fig. 5.** Analysis of VX680 sensitivity and protein expression. Cell lines are indicated as VX680 resistant (R), sensitive (S), and intermediately sensitive (M) and were chosen from the NSCLC panel to probe for the abundance and phosphorylation of key cell cycle proteins. As for erlotinib, IC-50 values were categorized into a quartile with high IC-50 values (R), a quartile with low IC-50 values (S) and in a group comprising the two quartiles with intermediate sensitivity (M). Nuclear extracts of VX680 sensitive cells showed increased phosphorylation of RB, nuclear extracts of VX680 resistant cells lacked expression of AURKA and were positive for CDK4. Nuclear extracts obtained from cell lines with intermediate sensitivity to VX680 were positive for various cell cycle proteins including AURKA and CDC2 (CDK1) but did not show strong RB phosphorylation. No direct comparison with RPPA data was carried out since RPPA was based on the analysis of total cell lysates.

presents a promising alternative over standard chemotherapy especially for well-defined subgroups of patients [9,3,7]. However, for the majority of targeted drugs useful guidelines and biomarker panels still need to be defined to make the next step towards clinical validation [35,11]. Solid cancers have accumulated many different genetic aberrations in multiple oncogenes and/or tumor suppressor genes [36]. Thus, in order to further improve a stratification of lung cancer patients for treatments with targeted drugs, our understanding of how genetic aberrations affect cellular signaling and how this correlates with drug sensitivity needs to be improved. For this reason, reverse phase protein microarrays were employed to analyze the proteomic architecture of signaling pathways in a panel of cell lines representing all types of NSCLC, and the NSCLC cell line panel chosen shows genomic aberrations characteristic for primary lung cancer [37]. Data analysis was based on correlating proteomic data with sensitivity towards commonly used anti-EGFR drugs as well as towards the aurora kinase inhibitor VX800.

### 4.1. Impact of genetic aberrations on signal transduction circuits

Oncogenic aberrations such as *EGFR*, *ERBB2*, *MET*, *PI3KCA*, *EML4-ALK*, *STK11*, *KRAS*, *NRAS*, *TP53*, and *BRAF* have previously been reported for the NSCLC cell line panel [13]. The hierarchal clustering of proteomic data, shown here, revealed the existence of pathway-specific clusters. For example, cell lines with high level activation of EGFR and ERBB2 formed a homogenous protein cluster which included 50% of NSCLC cell lines with *EGFR* gene amplifications and both *ERBB2* amplified NSCLC cell lines. Cluster formation in a targeted proteomic approach is certainly influenced by proteins and phosphoproteins chosen to represent a certain signaling node as in this instance, choosing numerous antibodies that recognize phosphoepitopes of EGFR or ERBB2. However, others have observed that ERBB2 stabilizes other ERBB family members [38] and thereby indicating that pathway activation profiling can hint towards synergistic effects on the protein level. Unsupervised learning of transcript data did correctly identify EGFR or ERBB amplification but did not detect synergistic effects between both receptors. This suggests that interactions existing on the proteomic level modulate the signaling response and might this way contribute to drive cancer. A property of the ERBB2/EGFR cell line cluster was low level activation of pro-survival proteins known from the PI3K/AKT signaling axis suggesting that tumors with constitutive signaling through EGFR and HER2 might progress without a need for high level activation of AKT signaling as pro-survival pathway. In conclusion, targeting the PI3K/AKT module might not present a therapeutically meaningful measure in tumors with an amplification of *EGFR* or *ERBB2*. In cancer, ERBB2 overexpression is highly correlated with drug resistance and ERBB2-amplified lung cancers revealed a high metastatic potential under standard chemotherapy. However, ERBB2 amplified NSCLC cell lines were highly sensitive towards treatment with the EGFR inhibitor PD168393 (Calu3) or with the dual EGFR/ERBB2 inhibitor lapatinib (Calu3, H1819). Both cell lines were characterized by high level ERBB2/EGFR phosphorylation suggesting a strong interaction between both receptors on a functional level as previously reported for the EGFR/ERBB2 receptor module [39]. Prediction of drug susceptibility based on information of genetic lesions, confirmed mutation of EGFR as the predominant factor of sensitivity towards treatment with erlotinib and other EGFR-targeting drugs [37].

A small number of lung cancers has been associated with mutations in phosphoinositide-3-kinase-catalytic α polypeptide (*PIK3CA*) [40]. In principle, mutations in the p110 catalytic subunit of PI3K leads to an autoactivation of the PI3K/AKT pathway by phosphorylating the pro-survival kinase AKT which this way activates cell growth, proliferation, survival, and malignant transformation [41,42]. The panel of proteins analyzed by RPPA did not indicate an association with the mutational status of *PIK3CA* and any pathway analyzed by RPPA, confirming findings made for the NCI 60 cancer cell line set [43] and in breast cancer tissues [44].

In cancer research, *RAS* presents a well-studied oncogene and its mutation has been shown to result in abnormal cell proliferation. KRAS, for example, is activated by point mutations most frequently affecting codons 12, 13, and 61. Mutations of *KRAS*, *NRAS*, and *BRAF* were found equally distributed across signaling pathway clusters that constituted the proteomic heatmap of NSCLC cell lines. Supervised learning was therefore used to identify proteins which might be associated with *KRAS* mutations. Proliferating cell nuclear antigen (PCNA) levels were significantly elevated in cell lines with *KRAS* mutations. Enhanced expression of PCNA is a general characteristic for fast proliferating cells and therefore most likely reflects the growth rate. Cells with mutated *KRAS* revealed reduced pEGFR phosphorylation and higher level expression of pro-survival proteins such as pAKT (S473) and PP2A. The contrary was seen in *EGFR* amplified cells, revealing higher level of EGFR phosphorylation and relatively lower levels of AKT phosphorylation and a downregulation of PP2A. In conclusion, a close association between PP2A expression and AKT activity might therefore link receptor phosphorylation and downstream signaling, suggesting that highly abundant PP2A might indicate a shift towards the PI3K/AKT axis. EGFR phosphorylation on Y1173 located to cluster P2 and was apparently not coregulated with EGFR phosphosites Y992, Y1086, and Y1068 of cluster P5. This finding is in line with clinical data obtained by immunohistochemistry on the EGFR phosphorylation showing that in contrast to a phosphorylation of pEGFR on Y1173, EGFR phosphorylation on Y1068 was highly correlated with clinical outcome of lung cancer patients and response towards small molecule drugs targeting EGFR [45]. The heatmap hierarchy confirmed that amplification of *EGFR*/*ERBB2* and mutations of the *RAS*/*BRAF* module are indeed mutually exclusive. It has been anticipated that both mutations result in a similar outcome on a functional level. *TP53* mutations were amply abundant in the NSCLC cell line panel, higher enriched in clusters C1 and C4 (60–66%) and less abundant in cluster C5 where only one out of five cell lines was *TP53* mutated.

Amplification of *EGFR* and *ERBB2* correlated with low SMAD2/3 and low β-Catenin levels. SMAD2 and SMAD3, members of the SMAD family

of signal transduction molecules, transmit TGF-β signals from the cell surface to the nucleus. According to the current understanding of SMAD signaling, SMAD2 and SMAD3 belong to the class of activating SMADs downstream of TGF-β receptor [46]. TGF-β signaling has been associated with tumor-suppressing as well as with tumor-promoting activities [47,48] and interpretation of a functional relevance of SMAD expression levels cannot easily be made. Furthermore, low SMAD2/3 and low level β-Catenin expression were seen in all cell lines with a RTK mutation or amplification. Downregulation of β-Catenin expression has been associated with cancer aggressiveness [49,50]. Hence, the basic understanding is that low level abundance of β-Catenin produces fragile cell–cell adhesions so that cells tend to dissociate more easily and this way increase the metastatic potential of cells. Taken together, downregulation of SMAD2/3 and β-Catenin seems to synergistically drive lung cancer progression.

### 4.2. Identification of drug sensitivity marker proteins

The introduction of targeted drugs to anticancer-therapies has been followed by an immense need to identify predictive markers. An association between drug sensitivity and genetic lesions has already been reported for the NSCLC cell line panel analyzed in this study [13]. Certain genetic aberrations such as *EGFR* mutation and *EGFR* amplification have been identified as predictive indicators of a response towards receptor tyrosine kinase targeting drugs. However, cellular response to a certain drug depends on the activation state of the targeted signaling node, particularly feedback regulation circuits which are not directly accessible by transcriptomics [51]. Proteomic profiles were analyzed to identify proteins associated with sensitivity towards a specific drug. Sensitivity towards erlotinib was highly significantly associated with total EGFR expression, high level EGFR phosphorylation on Y1068 and low level expression of PP2A.

Furthermore, in addition to high level expression of aurora kinase A, high-level phosphorylation of RB presents putative markers of VX680 sensitivity. A correlation between high levels of aurora kinase A and VX680 sensitivity has previously been reported in AML [52]. Targeting highly regulated cell cycle proteins seems to be a particular challenge for drug discovery and appears to be promising in conjunction with drugs that arrest cancer cells in a specific cell cycle phase.

This article has selected examples from NSCLC pathway activation profiling to illustrate that the RPPA technology presents a powerful platform for targeted proteomics that can advance our understanding of drug response in cancer. Results revealed that proteins identified as potential drug sensitivity markers might also be indicative of drug resistance when regulated in an inverse manner. In principle, knowledge obtained by systematic in vitro experimentation can be used further to achieve the goal of personalized medicine; thus, prediction of sensitivity towards certain drugs in tumors with defined genetic and proteomic signatures.

Supplementary data to this article can be found online at http://dx.doi.org/10.1016/j.bbapap.2013.11.017.

## Disclosure of potential conflicts of interest

Authors declare no potential conflicts of interest.

## Acknowledgements

The project was supported by the German Federal Ministry of Education and Research (BMBF) FKZ: 01EO1002, the program for medical genome research (01GS0890, 01GS0864, 01GS0898) as well as by the ERASySBio + project "LivSysiPS" (0315717C), the CancerSys-Project MYCNET (0316076C), and the eBio initiative, SYSMET-BC 0316168D. All authors are responsible for the content of this publication. Authors acknowledge Roman Thomas and his coworkers Martin Sos, Johannes Heuckmann, and Stephanie Heynck for providing cell line samples and information on the NSCLC cell line panel.

## References

[1] A. Jemal, F. Bray, M.M. Center, J. Ferlay, E. Ward, D. Forman, Global cancer statistics, CA Cancer J. Clin. 61 (2011) 69–90.
[2] W.K. Lam, N.W. White, M.M. Chan-Yeung, Lung cancer epidemiology and risk factors in Asia and Africa, Int. J. Tuberc. Lung. Dis. 8 (2004) 1045–1057.
[3] M.J. Thun, L.M. Hannan, L.L. Adams-Campbell, P. Boffetta, J.E. Buring, D. Feskanich, W.D. Flanders, S.H. Jee, K. Katanoda, L.N. Kolonel, I.M. Lee, T. Marugame, J.R. Palmer, E. Riboli, T. Sobue, E. Avila-Tang, L.R. Wilkens, J.M. Samet, Lung cancer occurrence in never-smokers: an analysis of 13 cohorts and 22 cancer registry studies, PLoS Med. 5 (2008) e185.
[4] R. Salgia, A.T. Skarin, Molecular abnormalities in lung cancer, J. Clin. Oncol. 16 (1998) 1207–1217.
[5] R.S. Herbst, J.V. Heymach, S.M. Lippman, Lung cancer, N. Engl. J. Med. 359 (2008) 1367–1380.
[6] P.A. Janne, J.A. Engelman, B.E. Johnson, Epidermal growth factor receptor mutations in non-small-cell lung cancer: implications for treatment and tumor biology, J. Clin. Oncol. 23 (2005) 3227–3234.
[7] R. Feld, S.S. Sridhar, F.A. Shepherd, J.A. Mackay, W.K. Evans, C. Lung Cancer Disease Site Group of Cancer Care Ontario's Program in Evidence-based, use of the epidermal growth factor receptor inhibitors gefitinib and erlotinib in the treatment of non-small cell lung cancer: a systematic review, J. Thorac. Oncol. 1 (2006) 367–376.
[8] F. Cappuzzo, F.R. Hirsch, E. Rossi, S. Bartolini, G.L. Ceresoli, L. Bemis, J. Haney, S. Witta, K. Danenberg, I. Domenichini, V. Ludovini, E. Magrini, V. Gregorc, C. Doglioni, A. Sidoni, M. Tonato, W.A. Franklin, L. Crino, P.A. Bunn Jr., M. Varella-Garcia, Epidermal growth factor receptor gene and protein and gefitinib sensitivity in non-small-cell lung cancer, J. Natl. Cancer Inst. 97 (2005) 643–655.
[9] G.C. Chang, C.M. Tsai, K.C. Chen, C.J. Yu, J.Y. Shih, T.Y. Yang, C.P. Lin, J.Y. Hsu, C.H. Chiu, R.P. Perng, P.C. Yang, C.H. Yang, Predictive factors of gefitinib antitumor activity in East Asian advanced non-small cell lung cancer patients, J. Thorac. Oncol. 1 (2006) 520–525.
[10] F.R. Hirsch, P.A. Bunn Jr., Epidermal growth factor receptor inhibitors in lung cancer: smaller or larger molecules, selected or unselected populations? J. Clin. Oncol. 23 (2005) 9044–9047.
[11] T.J. Lynch, D.W. Bell, R. Sordella, S. Gurubhagavatula, R.A. Okimoto, B.W. Brannigan, P.L. Harris, S.M. Haserlat, J.G. Supko, F.G. Haluska, D.N. Louis, D.C. Christiani, J. Settleman, D.A. Haber, Activating mutations in the epidermal growth factor receptor underlying responsiveness of non-small-cell lung cancer to gefitinib, N. Engl. J. Med. 350 (2004) 2129–2139.
[12] J.G. Paez, P.A. Janne, J.C. Lee, S. Tracy, H. Greulich, S. Gabriel, P. Herman, F.J. Kaye, N. Lindeman, T.J. Boggon, K. Naoki, H. Sasaki, Y. Fujii, M.J. Eck, W.R. Sellers, B.E. Johnson, M. Meyerson, EGFR mutations in lung cancer: correlation with clinical response to gefitinib therapy, Science 304 (2004) 1497–1500.
[13] M.L. Sos, K. Michel, T. Zander, J. Weiss, P. Frommolt, M. Peifer, D. Li, R. Ullrich, M. Koker, F. Fischer, T. Shimamura, D. Rauh, C. Mermel, S. Fischer, I. Stuckrath, S. Heynck, R. Beroukhim, W. Lin, W. Winckler, K. Shah, T. LaFramboise, W.F. Moriarty, M. Hanna, L. Tolosi, J. Rahnenfuhrer, R. Verhaak, D. Chiang, G. Getz, M. Hellmich, J. Wolf, L. Girard, M. Peyton, B.A. Weir, T.H. Chen, H. Greulich, J. Barretina, G.I. Shapiro, L.A. Garraway, A.F. Gazdar, J.D. Minna, M. Meyerson, K.K. Wong, R.K. Thomas, Predicting drug susceptibility of non-small cell lung cancers based on genetic lesions, J. Clin. Invest. 119 (2009) 1727–1740.
[14] M.L. Sos, R.K. Thomas, Systematically linking drug susceptibility to cancer genome aberrations, Cell Cycle 8 (2009) 3652–3656.
[15] R. Tibes, Y. Qiu, Y. Lu, B. Hennessy, M. Andreeff, G.B. Mills, S.M. Kornblau, Reverse phase protein array: validation of a novel proteomic technology and utility for analysis of primary leukemia specimens and hematopoietic stem cells, Mol. Cancer Ther. 5 (2006) 2512–2521.
[16] B.T. Hennessy, Y. Lu, A.M. Gonzalez-Angulo, M.S. Carey, S. Myhre, Z. Ju, M.A. Davies, W. Liu, K. Coombes, F. Meric-Bernstam, I. Bedrosian, M. McGahren, R. Agarwal, F. Zhang, J. Overgaard, J. Alsner, R.M. Neve, W.L. Kuo, J.W. Gray, A.L. Borresen-Dale, G.B. Mills, A technical assessment of the utility of reverse phase protein arrays for the study of the functional proteome in non-microdissected human breast cancers, Clin. Proteomics 6 (2010) 129–151.
[17] C.P. Paweletz, L. Charboneau, V.E. Bichsel, N.L. Simone, T. Chen, J.W. Gillespie, M.R. Emmert-Buck, M.J. Roth, I.E. Petricoin, L.A. Liotta, Reverse phase protein microarrays which capture disease progression show activation of pro-survival pathways at the cancer invasion front, Oncogene 20 (2001) 1981–1989.
[18] M. Pawlak, E. Schick, M.A. Bopp, M.J. Schneider, P. Oroszlan, M. Ehrat, Zeptosens' protein microarrays: a novel high performance microarray platform for low abundance protein analysis, Proteomics 2 (2002) 383–393.
[19] J.D. Wulfkuhle, J.A. Aquino, V.S. Calvert, D.A. Fishman, G. Coukos, L.A. Liotta, E.F. Petricoin III, Signal pathway profiling of ovarian cancer from human tissue specimens using reverse-phase protein microarrays, Proteomics 3 (2003) 2085–2090.
[20] S. Nishizuka, L. Charboneau, L. Young, S. Major, W.C. Reinhold, M. Waltham, H. Kouros-Mehr, K.J. Bussey, J.K. Lee, V. Espina, P.J. Munson, E. Petricoin III, L.A. Liotta, J.N. Weinstein, Proteomic profiling of the NCI-60 cancer cell lines using new high-density reverse-phase lysate microarrays, Proc. Natl. Acad. Sci. U. S. A. 100 (2003) 14229–14234.
[21] C. Loebke, H. Sueltmann, C. Schmidt, F. Henjes, S. Wiemann, A. Poustka, U. Korf, Infrared-based protein detection arrays for quantitative proteomics, Proteomics 7 (2007) 558–564.

[22] L. Zhang, Q. Wei, L. Mao, W. Liu, G.B. Mills, K. Coombes, Serial dilution curve: a new method for analysis of reverse phase protein array data, Bioinformatics 25 (2009) 650–654.
[23] H.A. Mannsperger, S. Gade, F. Henjes, T. Beissbarth, U. Korf, RPPanalyzer: analysis of reverse-phase protein array data, Bioinformatics 26 (2010) 2202–2203.
[24] S. Troncale, A. Barbet, L. Coulibaly, E. Henry, B. He, E. Barillot, T. Dubois, P. Hupe, L. de Koning, NormaCurve: a SuperCurve-based method that simultaneously quantifies and normalizes reverse phase protein array data, PLoS One 7 (2012) e38686.
[25] B. Spurrier, S. Ramalingam, S. Nishizuka, Reverse-phase protein lysate microarrays for cell signaling analysis, Nat. Protoc. 3 (2008) 1796–1808.
[26] H.A. Mannsperger, S. Uhlmann, C. Schmidt, S. Wiemann, O. Sahin, U. Korf, RNAi-based validation of antibodies for reverse phase protein arrays, Proteome Sci. 8 (2010) 69.
[27] R.K. Thomas, B. Weir, M. Meyerson, Genomic approaches to lung cancer, Clin. Cancer Res. 12 (2006) 4384s–4391s.
[28] B. Schwanhausser, D. Busse, N. Li, G. Dittmar, J. Schuchhardt, J. Wolf, W. Chen, M. Selbach, Global quantification of mammalian gene expression control, Nature 473 (2011) 337–342.
[29] U. Korf, S. Derdak, A. Tresch, F. Henjes, S. Schumacher, C. Schmidt, B. Hahn, W.D. Lehmann, A. Poustka, T. Beissbarth, U. Klingmuller, Quantitative protein microarrays for time-resolved measurements of protein phosphorylation, Proteomics 8 (2008) 4603–4612.
[30] J. Barretina, G. Caponigro, N. Stransky, K. Venkatesan, A.A. Margolin, S. Kim, C.J. Wilson, J. Lehar, G.V. Kryukov, D. Sonkin, A. Reddy, M. Liu, L. Murray, M.F. Berger, J.E. Monahan, P. Morais, J. Meltzer, A. Korejwa, J. Jane-Valbuena, F.A. Mapa, J. Thibault, E. Bric-Furlong, P. Raman, A. Shipway, I.H. Engels, J. Cheng, G.K. Yu, J. Yu, P. Aspesi Jr., M. de Silva, K. Jagtap, M.D. Jones, L. Wang, C. Hatton, E. Palescandolo, S. Gupta, S. Mahan, C. Sougnez, R.C. Onofrio, T. Liefeld, L. MacConaill, W. Winckler, M. Reich, N. Li, J.P. Mesirov, S.B. Gabriel, G. Getz, K. Ardlie, V. Chan, V.E. Myer, B.L. Weber, J. Porter, M. Warmuth, P. Finan, J.L. Harris, M. Meyerson, T.R. Golub, M.P. Morrissey, W.R. Sellers, R. Schlegel, L.A. Garraway, The Cancer Cell Line Encyclopedia enables predictive modelling of anticancer drug sensitivity, Nature 483 (2012) 603–607.
[31] D.R. Xu, S. Huang, Z.J. Long, J.J. Chen, Z.Z. Zou, J. Li, D.J. Lin, Q. Liu, Inhibition of mitotic kinase Aurora suppresses Akt-1 activation and induces apoptotic cell death in all-trans retinoid acid-resistant acute promyelocytic leukemia cells, J. Transl. Med. 9 (2011) 74.
[32] S. Medves, J.B. Demoulin, Tyrosine kinase gene fusions in cancer: translating mechanisms into targeted therapies, J. Cell. Mol. Med. 16 (2012) 237–248.
[33] G.V. Scagliotti, S. Novello, The role of the insulin-like growth factor signaling pathway in non-small cell lung cancer and other solid tumors, Cancer Treat. Rev. 38 (2012) 292–302.
[34] E. Castellano, J. Downward, RAS interaction with PI3K: more than just another effector pathway, Genes Cancer 2 (2011) 261–274.
[35] L.V. Sequist, D.W. Bell, T.J. Lynch, D.A. Haber, Molecular predictors of response to epidermal growth factor receptor antagonists in non-small-cell lung cancer, J. Clin. Oncol. 25 (2007) 587–595.
[36] D. Hanahan, R.A. Weinberg, Hallmarks of cancer: the next generation, Cell 144 (2011) 646–674.
[37] M.L. Sos, S. Fischer, R. Ullrich, M. Peifer, J.M. Heuckmann, M. Koker, S. Heynck, I. Stuckrath, J. Weiss, F. Fischer, K. Michel, A. Goel, L. Regales, K.A. Politi, S. Perera, M. Getlik, L.C. Heukamp, S. Ansen, T. Zander, R. Beroukhim, H. Kashkar, K.M. Shokat, W.R. Sellers, D. Rauh, C. Orr, K.P. Hoeflich, L. Friedman, K.K. Wong, W. Pao, R.K. Thomas, Identifying genotype-dependent efficacy of single and combined PI3K- and MAPK-pathway inhibition in cancer, Proc. Natl. Acad. Sci. U. S. A. 106 (2009) 18351–18356.
[38] B.S. Hendriks, H.S. Wiley, D. Lauffenburger, HER2-mediated effects on EGFR endosomal sorting: analysis of biophysical mechanisms, Biophys. J. 85 (2003) 2732–2745.
[39] O. Sahin, H. Frohlich, C. Lobke, U. Korf, S. Burmester, M. Majety, J. Mattern, I. Schupp, C. Chaouiya, D. Thieffry, A. Poustka, S. Wiemann, T. Beissbarth, D. Arlt, Modeling ERBB receptor-regulated G1/S transition to find novel targets for de novo trastuzumab resistance, BMC Syst. Biol. 3 (2009) 1.
[40] L. Ding, G. Getz, D.A. Wheeler, E.R. Mardis, M.D. McLellan, K. Cibulskis, C. Sougnez, H. Greulich, D.M. Muzny, M.B. Morgan, L. Fulton, R.S. Fulton, Q. Zhang, M.C. Wendl, M.S. Lawrence, D.E. Larson, K. Chen, D.J. Dooling, A. Sabo, A.C. Hawes, H. Shen, S.N. Jhangiani, L.R. Lewis, O. Hall, Y. Zhu, T. Mathew, Y. Ren, J. Yao, S.E. Scherer, K. Clerc, G.A. Metcalf, B. Ng, A. Milosavljevic, M.L. Gonzalez-Garay, J.R. Osborne, R. Meyer, X. Shi, Y. Tang, D.C. Koboldt, L. Lin, R. Abbott, T.L. Miner, C. Pohl, G. Fewell, C. Haipek, H. Schmidt, B.H. Dunford-Shore, A. Kraja, S.D. Crosby, C.S. Sawyer, T. Vickery, S. Sander, J. Robinson, W. Winckler, J. Baldwin, L.R. Chirieac, A. Dutt, T. Fennell, M. Hanna, B.E. Johnson, R.C. Onofrio, R.K. Thomas, G. Tonon, B.A. Weir, X. Zhao, L. Ziaugra, M.C. Zody, T. Giordano, M.B. Orringer, J.A. Roth, M.R. Spitz, I.I. Wistuba, B. Ozenberger, P.J. Good, A.C. Chang, D.G. Beer, M.A. Watson, M. Ladanyi, S. Broderick, A. Yoshizawa, W.D. Travis, W. Pao, M.A. Province, G.M. Weinstock, H.E. Varmus, S.B. Gabriel, E.S. Lander, R.A. Gibbs, M. Meyerson, R.K. Wilson, Somatic mutations affect key pathways in lung adenocarcinoma, Nature 455 (2008) 1069–1075.
[41] J. Brognard, A.S. Clark, Y. Ni, P.A. Dennis, Akt/protein kinase B is constitutively active in non-small cell lung cancer cells and promotes cellular survival and resistance to chemotherapy and radiation, Cancer Res. 61 (2001) 3986–3997.
[42] B. Karakas, K.E. Bachman, B.H. Park, Mutation of the PIK3CA oncogene in human cancers, Br. J. Cancer 94 (2006) 455–459.
[43] B.T. Hennessy, D.L. Smith, P.T. Ram, Y. Lu, G.B. Mills, Exploiting the PI3K/AKT pathway for cancer drug discovery, Nat. Rev. Drug Discov. 4 (2005) 988–1004.
[44] E.S. Park, R. Rabinovsky, M. Carey, B.T. Hennessy, R. Agarwal, W. Liu, Z. Ju, W. Deng, Y. Lu, H.G. Woo, S.B. Kim, J.H. Cheong, L.A. Garraway, J.N. Weinstein, G.B. Mills, J.S. Lee, M.A. Davies, Integrative analysis of proteomic signatures, mutations, and drug responsiveness in the NCI 60 cancer cell line set, Mol. Cancer Ther. 9 (2010) 257–267.
[45] F. Wang, S. Wang, Z. Wang, J. Duan, T. An, J. Zhao, H. Bai, J. Wang, C. Key Laboratory of R. Translational, Phosphorylated EGFR expression may predict outcome of EGFR-TKIs therapy for the advanced NSCLC patients with wild-type EGFR, J. Exp. Clin. Cancer Res. 31 (2012) 65.
[46] K. Stemke-Hale, A.M. Gonzalez-Angulo, A. Lluch, R.M. Neve, W.L. Kuo, M. Davies, M. Carey, Z. Hu, Y. Guan, A. Sahin, W.F. Symmans, L. Pusztai, L.K. Nolden, H. Horlings, K. Berns, M.C. Hung, M.J. van de Vijver, V. Valero, J.W. Gray, R. Bernards, G.B. Mills, B.T. Hennessy, An integrative genomic and proteomic analysis of PIK3CA, PTEN, and AKT mutations in breast cancer, Cancer Res. 68 (2008) 6084–6091.
[47] C.H. Heldin, K. Miyazono, P. ten Dijke, TGF-beta signalling from cell membrane to nucleus through SMAD proteins, Nature 390 (1997) 465–471.
[48] M.P. de Caestecker, E. Piek, A.B. Roberts, Role of transforming growth factor-beta signaling in cancer, J. Natl. Cancer Inst. 92 (2000) 1388–1402.
[49] A. Damalas, S. Kahan, M. Shtutman, A. Ben-Ze'ev, M. Oren, Deregulated beta-catenin induces a p53- and ARF-dependent growth arrest and cooperates with Ras in transformation, EMBO J. 20 (2001) 4912–4922.
[50] M.P. Ebert, J. Yu, J. Hoffmann, A. Rocco, C. Rocken, S. Kahmann, O. Muller, M. Korc, J.J. Sung, P. Malfertheiner, Loss of beta-catenin expression in metastatic gastric cancer, J. Clin. Oncol. 21 (2003) 1708–1714.
[51] K.R. Calvo, L.A. Liotta, E.F. Petricoin, Clinical proteomics: from biomarker discovery and cell signaling profiles to individualized personal therapy, Biosci. Rep. 25 (2005) 107–125.
[52] X.F. Huang, S.K. Luo, J. Xu, J. Li, D.R. Xu, L.H. Wang, M. Yan, X.R. Wang, X.B. Wan, F.M. Zheng, Y.X. Zeng, Q. Liu, Aurora kinase inhibitory VX-680 increases Bax/Bcl-2 ratio and induces apoptosis in Aurora-A-high acute myeloid leukemia, Blood 111 (2008) 2854–2865.